Supporting Information

Fast-response fiber organic electrochemical transistor with vertical channel design for electrophysiological monitoring

*Jiawei Chen†, Yuan Fang†, Jianyou Feng, Xiang Shi, Jinyan Li, Shuzhuang Wang, Songlin Zhang, Huisheng Peng, and Xuemei Sun**

State Key Laboratory of Molecular Engineering of Polymers, Department of Macromolecular Science, Institute of Fiber Materials and Devices, and Laboratory of Advanced Materials, Fudan University, Shanghai, 200438, China.
E-mail: sunxm@fudan.edu.cn.

†These authors contributed equally to this work.

Experimental Section/Methods

Materials

Nylon fibers were purchased from Toray Industries, Inc. Polyethylene terephthalate (PET) tapes were purchased from Mingchao Co., Ltd. Poly(3,4-ethylene dioxythiophene):poly(styrene sulfonate) (PEDOT:PSS) aqueous dispersion (Clevios PH1000) was purchased from Heraeus. Ethylene glycol was purchased from Sinopharm Chemical Reagent Co., Ltd. 3-glycidoxypropyltrimethoxysilane was purchased from Alfa Aesar. Fluorocarbon surfactant (FS-63) was purchased from Dupont Co. Phosphate-buffered saline (PBS) was purchased from Solarbio Science and Technology Co., Ltd. All other standard reagents were purchased from Sinopharm Chemical Reagent Co., Ltd.

Preparation of Carbon Nanotube Fibers

The carbon nanotube (CNT) sheets were first synthesized using the floating catalyst chemical vapor deposition method.[1] These sheets were then twisted into bundles to fabricate the CNT fibers, with eight sheets combined for each fiber.

Fabrication of Fiber Vertical OECTs (F-vOECTs)

Thermal evaporation was used to deposit 5-nm Cr/100-nm Au layers onto both nylon fibers and PET tapes. To achieve uniform Au coverage, deposition was conducted on both sides of the fixed fibers. Subsequently, the nylon/Cr/Au fiber was suspended, and the PET/Cr/Au tape was adhered to the curved surface of the fiber. The tape was then carefully folded under tension to encase the fiber. The assembly was subjected to twenty compression cycles using polydimethylsiloxane elastomer sheets to enhance interfacial adhesion between the fiber and film, followed by precise trimming to configure the stepped source/drain fiber. For channel fabrication, the formulation of PEDOT:PSS dispersion (1.1–1.3% solid content) was optimized by incorporating 0.05 wt% fluorocarbon surfactant (FS-63) to lower the surface tension, 1 wt% 3-glycidoxypropyltrimethoxysilane for cross-linking, and 10 wt% ethylene glycol to enhance conductivity. This optimized mixture was then concentrated to 40% of its original mass at 100°C in an oil bath, improving the film formation on the fiber substrate. The pristine source/drain fibers were then dip-coated in this concentrated PEDOT:PSS slurry at a rate of 300 mm/min, achieving channel thicknesses of 3 μm, 6 μm, and 12 μm after one, three, and six coating cycles, respectively. Since the film

thickness depends on the solution viscosity, shear rate, and number of dip-coating, this process allows for precise and reproducible control of the PEDOT:PSS layer properties. Furthermore, by selecting nylon fibers with varying diameters as the substrate, source/drain fibers with assorted diameters can be fabricated using the same methodology. Post-coating, the fibers were annealed in an argon atmosphere at 140°C for one hour to further improve the conductivity of the PEDOT:PSS. Non-channel areas were insulated by coating with a styrene-ethylene-butylene-styrene (SEBS) solution (10 wt%, 3 μL). The CNT fiber tip was masked with paper tape, and parylene C was deposited using a vacuum vapor deposition system. Upon removal of the tape, the patterned, parylene C-insulated CNT fiber was obtained, serving as the gate fiber. Finally, the source/drain fiber and gate fiber are wound together to assemble the fiber vertical OECT (F-vOECT).

Characterization

The structure and morphology of electrodes and devices were characterized by field emission scanning electron microscopy (Zeiss Ultra 55). The electrical properties of all devices were assessed in 0.01 M phosphate-buffered saline (PBS). Comprehensive electrical characterization, including output, transfer, response time, and cyclic switching behaviors of the F-vOECTs, was conducted using a Keysight semiconductor device analyzer (B1500A). The distance between the source/drain fiber and the gate fiber was set to 1 cm. For the output characteristic, the drain voltage (V_D) ranged from 0 to -0.8 V, and the gate voltage (V_G) ranged from 0 to 0.6 V in increments of 0.1 V. For the transfer characteristic, V_D was set at -0.6 V, and V_G was set from 0 to 1.1 V. The response time was determined by the period during which the I_{DS} change reached 90% of its maximum value upon maintaining V_D and switching V_G. In cyclic switching tests, V_D was set to -0.6 V, with V_G pulsing rapidly between 0 and 0.5 V. The AC impedance test was conducted using an electrical workstation (CHI660e, CH Instruments Inc.) with a three-electrode system comprising Ag/AgCl, Pt wire, and CNT fiber gate as the reference, counter, and working electrodes, respectively, across a frequency range of 1 Hz to 100,000 Hz. To standardize the bending process, the F-vOECTs were subjected to cyclic bending using a universal testing machine. Polymethyl methacrylate rods of varied diameters were utilized to adjust the bending radius.

In Vitro Testing of Simulated Electrocardiogram

Simulated electrocardiogram (ECG) waveforms were applied to the gate of the F-

vOECT using a Keysight B1500A in 0.01 M PBS, with V_D set at -0.6 V. The V_G curve was directly amplified and output by the instrument, while the amplification results of the F-vOECTs were derived from measurements of the drain-source current (I_{DS}). Two types of OECTs were fabricated for evaluation: a fast-response OECT with a 75 μm fiber diameter and 3 μm thicknesses for both PET film and PEDOT:PSS layer and a slow-response OECT with a 180 μm fiber diameter and the same thickness parameters. All signals were acquired without additional filtering.

In Vivo Monitoring of Electrocardiogram

The animal experiment protocols received approval from the Animal Experimentation Committee of Fudan University (approval number: SYXK2020-0032). All the experimental rats were managed according to guidelines for the care and use of experimental animals established by the National Institutes of Health and Fudan University. Experimental rats (SD, male, 8 weeks old) were purchased from Beijing Vital River Laboratory Animal Technology Co., Ltd. Comprehensive preoperative cleansing was undertaken to ensure a sterile environment. Rats were anesthetized with 1.5% isoflurane and positioned for surgery. With the assistance of a syringe, the source/drain fiber and gate fiber were subcutaneously implanted into the arm and chest regions of the rat, respectively, maintaining a distance of 1 cm between them. The implants were secured with tissue adhesive (3M) to prevent displacement during the experiment. Electrical connections were established using the Keysight B1500A, and the I_{DS} was measured *in vivo* with a V_D of -0.6 V and zero gate bias. The ECG of normal rats was then recorded under these conditions. Acute atrioventricular (AV) block was induced by intravenous administration of diltiazem (40 mg in 1 ml saline).[2] For long-term ECG monitoring, recordings were taken daily from Day 0 through Day 7.

Biocompatibility of F-vOECTs

After implantation of the F-vOECT for one week, rats were euthanized. Tissue samples from the skin with implanted devices and major organs (heart, liver, spleen, lung, and kidney), were excised and fixed in a 4% paraformaldehyde solution. These samples were embedded in paraffin wax and sectioned into 6 μm slices using a microtome (Leica RM2016, Leica Microsystems). The sections underwent H&E and immunofluorescence staining following standard procedures. For immunohistochemical staining, antigen retrieval was conducted using citrate buffer solution (pH 6.0), and sections were blocked with BSA for 30 minutes. Anti-CD68

(1:100, GB113109, Servicebio) served as the primary antibody, while Alexa Fluor® 488-conjugated goat anti-rabbit IgG (H+L) (1:400, GB25303, Servicebio) was used as the secondary antibody. Cell nuclei were stained with 4′,6-diamidino-2-phenylindole (DAPI, G1012, Servicebio). The stained sections were observed with NIKON ECLIPSE C1 (Nikon) and Pannoramic MIDI (3DHISTECH Ltd.).

Statistical analysis

Statistical evaluations were performed using GraphPad Prism 9.0. Data are expressed as mean ± standard deviation. Differences among groups were analyzed using unpaired two-tailed *t*-tests. Significance levels are indicated as: n.s., not significant ($P > 0.05$); *$P < 0.05$; **$P < 0.01$; ***$P < 0.005$; ****$P < 0.001$.

References

1. L. Wang, S. Xie, Z. Wang, F. Liu, Y. Yang, C. Tang, X. Wu, P. Liu, Y. Li, H. Saiyin, S. Zheng, X. Sun, F. Xu, H. Yu and H. Peng, *Nat. Biomed. Eng.*, 2020, **4**, 159-171.
2. H. Choi, Y. Kim, S. Kim, H. Jung, S. Lee, K. Kim, H.-S. Han, J. Y. Kim, M. Shin and D. Son, *Nat. Electron.*, 2023, **6**, 779-789.

Supplementary Figures

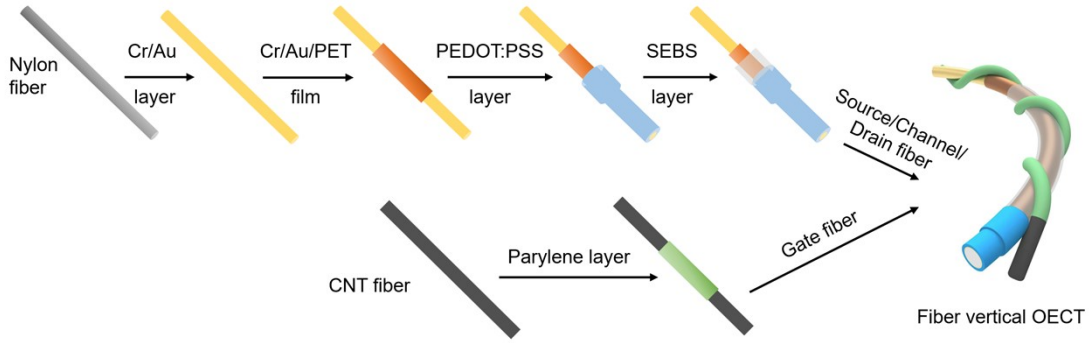

Fig. S1. Schematic illustration of the preparation process for the fiber vertical organic electrochemical transistor.

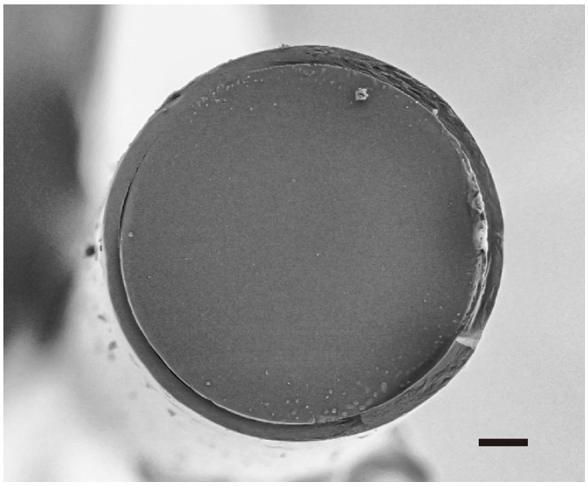

Fig. S2. Cross-sectional scanning electron microscopy image showcasing the uniform coating of PEDOT:PSS on the source/drain fiber tip. Scale bar, 10 μm.

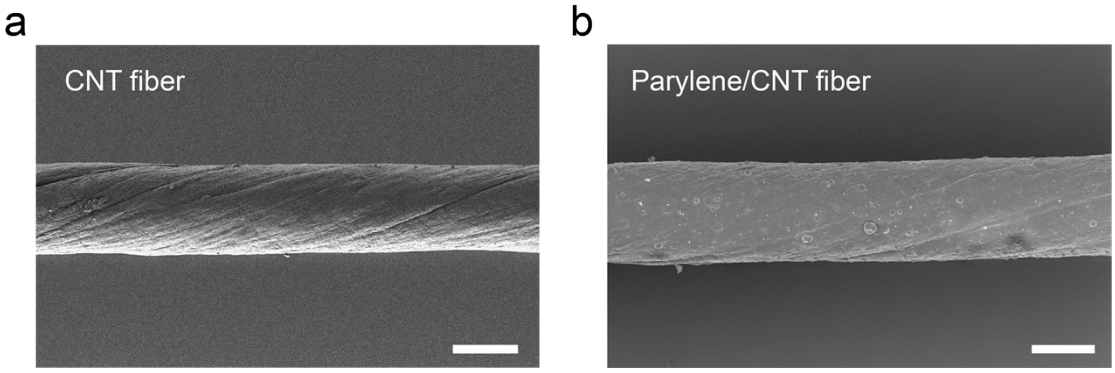

Fig. S3. Scanning electron microscope image of a CNT fiber gate electrode, showing (a) the exposed CNT fiber tip and (b) the parylene-insulated part. Scale bars, 50 μm.

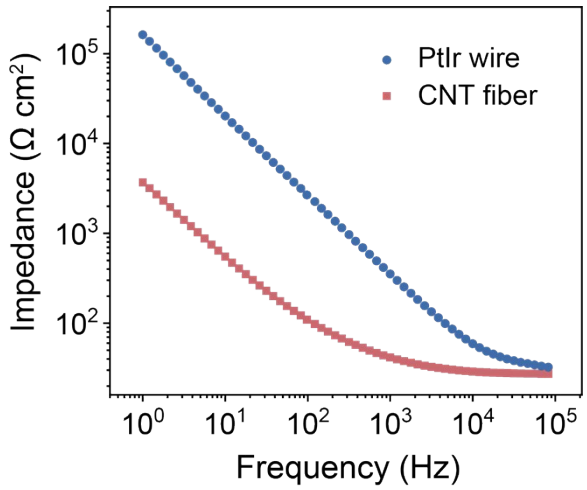

Fig. S4. Specific impedance spectra of PtIr wire and CNT fiber.

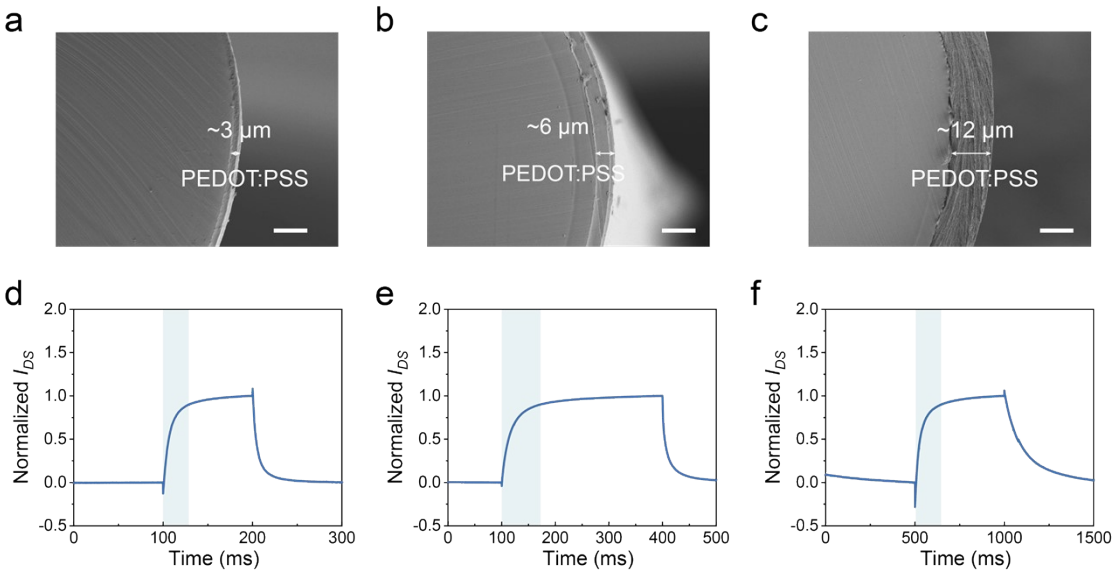

Fig. S5. Scanning electron microscope images display the channel structures of F-vOECTs with (a-c) varying thicknesses of PEDOT:PSS layers and (d-f) the corresponding response behavior of these devices (d_{film} of 3 μm, D_{fiber} of 180 μm) of (a, d) 3 μm, (b, e) 6 μm, and (c, f) 12 μm. Scale bars, 10 μm.

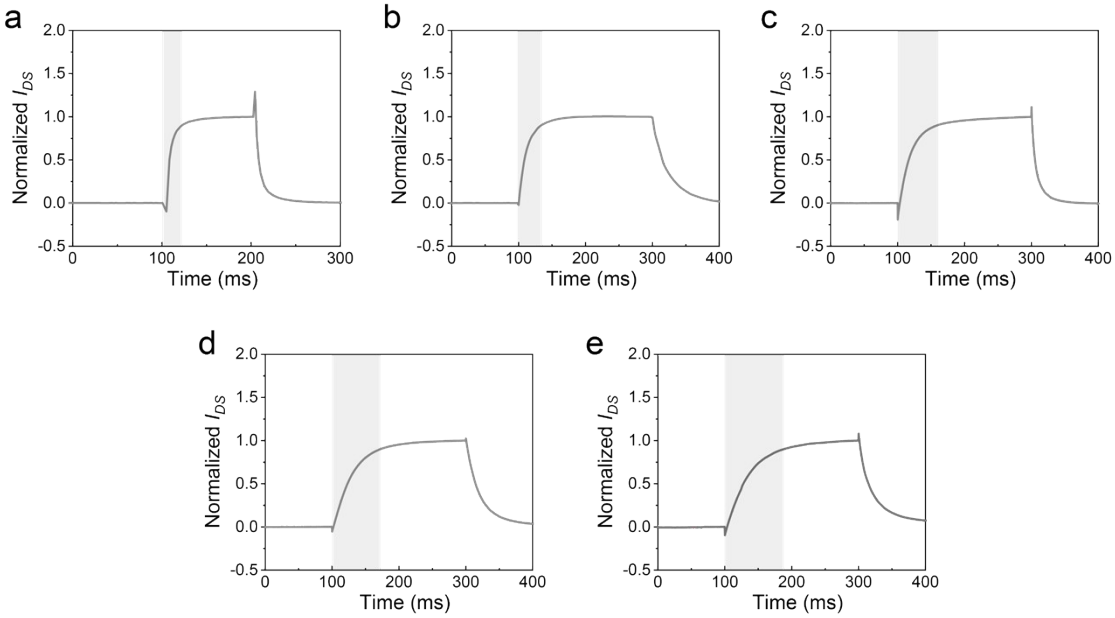

Fig. S6. Response behavior of the F-vOECTs (d_{film} of 3 μm, d of 3 μm) with fibers of varying diameters of (a) 100 μm, (b) 180 μm, (c) 300 μm, (d) 400 μm, and (e) 500 μm.

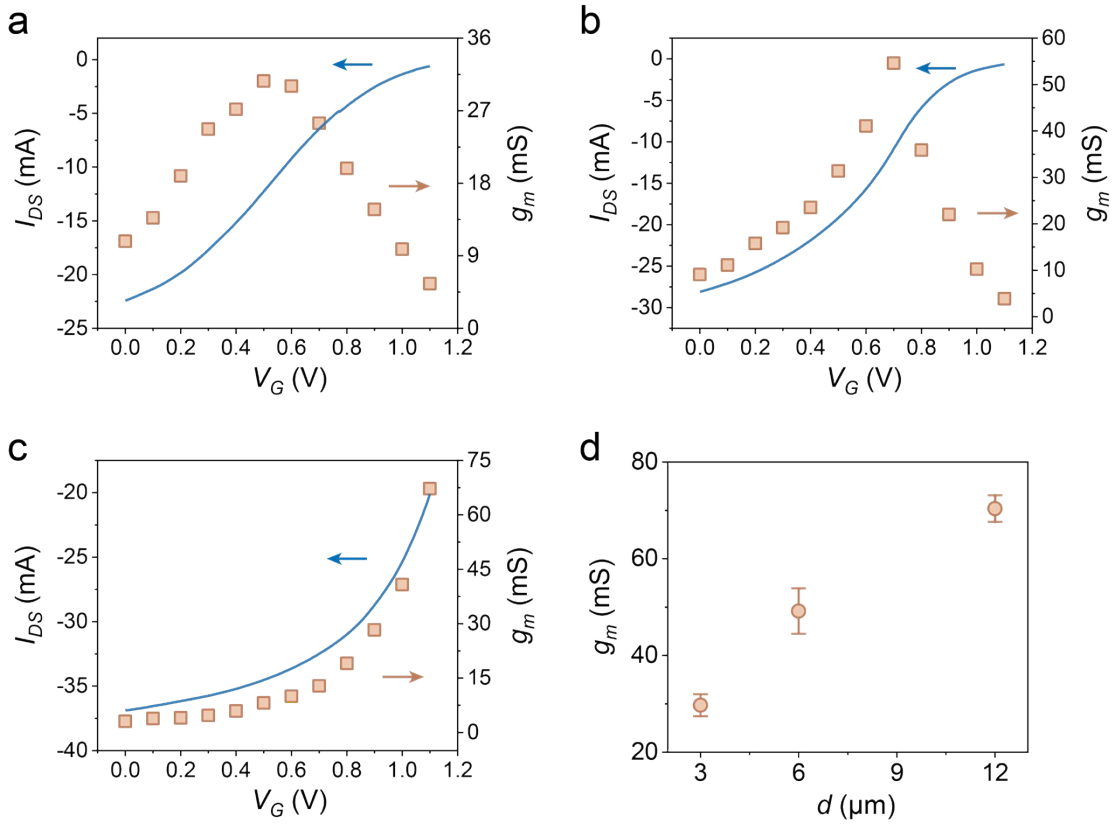

Fig. S7. Transfer characteristics of the F-vOECTs (d_{film} of 3 μm, D_{fiber} of 180 μm) with varying thicknesses of PEDOT:PSS layers of (a) 3 μm, (b) 6 μm, and (c) 12 μm. Panel (d) illustrates the dependence of transconductance (g_m) on PEDOT:PSS layer thickness (d) (n = 3, mean ± s.d.).

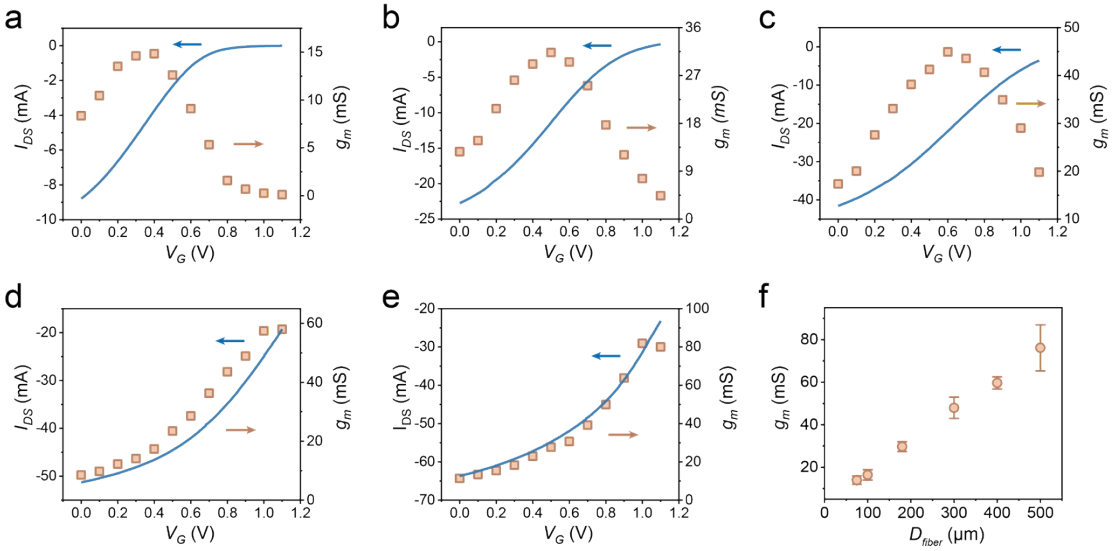

Fig. S8. Transfer characteristics of the F-vOECTs (d_{film} of 3 μm, d of 3 μm) with varying fiber diameters of (a) 100 μm, (b) 180 μm, (c) 300 μm, (d) 400 μm, and (e) 500 μm. Panel (f) shows the dependence of transconductance (g_m) on fiber diameter (D_{fiber}) (n = 3, mean ± s.d.).

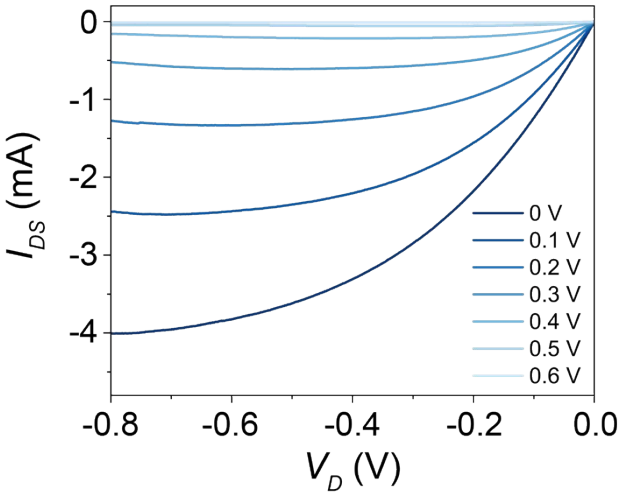

Fig. S9. Output curves of the F-vOECT (d_{film} of 3 μm, d of 3 μm, D_{fiber} of 75 μm) in 0.01 M PBS electrolyte.

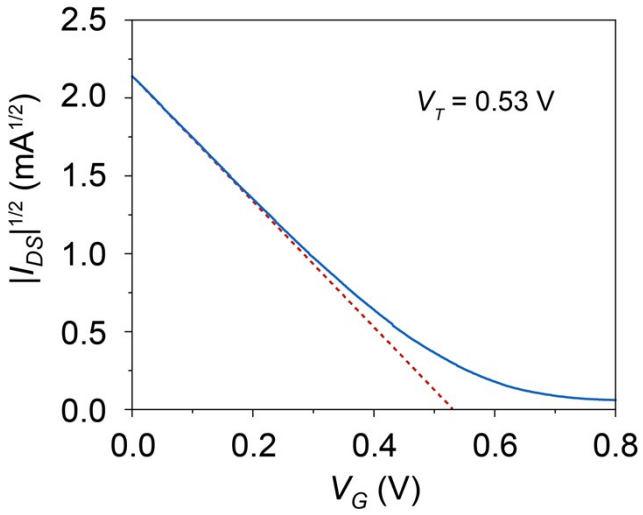

Fig. S10. Square root of the drain current as a function of gate voltage used to determine the threshold voltage.

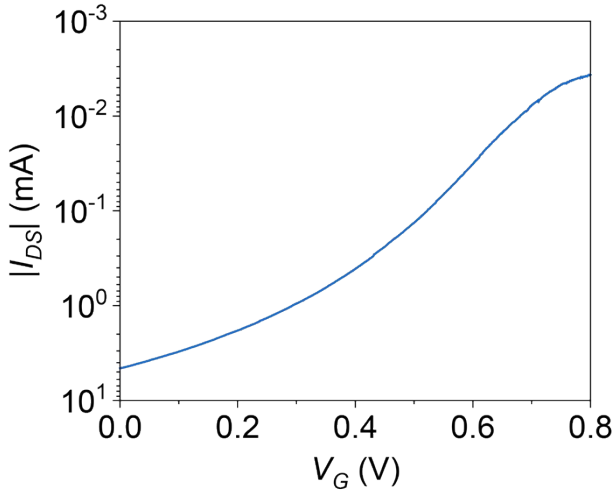

Fig. S11. Transfer curve of the F-vOECT (d_{film} of 3 μm, d of 3 μm, D_{fiber} of 75 μm) in the logarithmic scale for calculating the on-off current ratio. The drain current drops from 4.57 mA at V_G = 0 V, to 3.66 μA at V_G = 0.8 V.

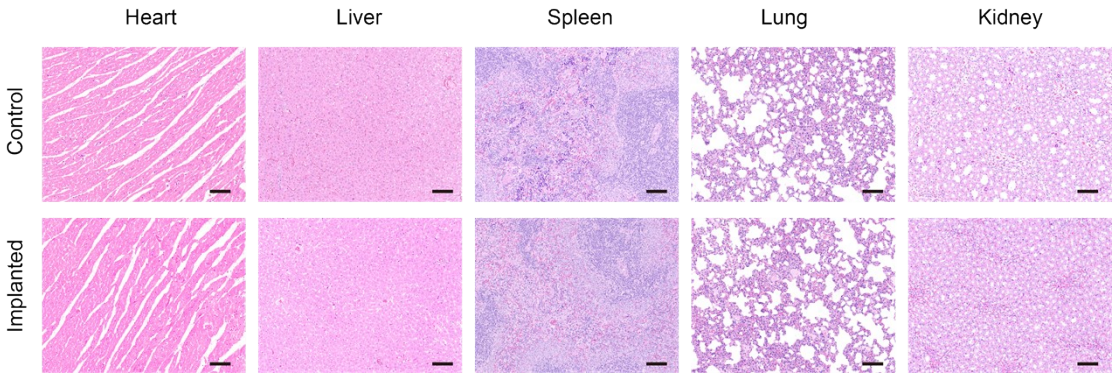

Fig. S12. H&E staining of major organs from rats implanted with F-vOECT for one week and controls. Scale bar, 100 μm.

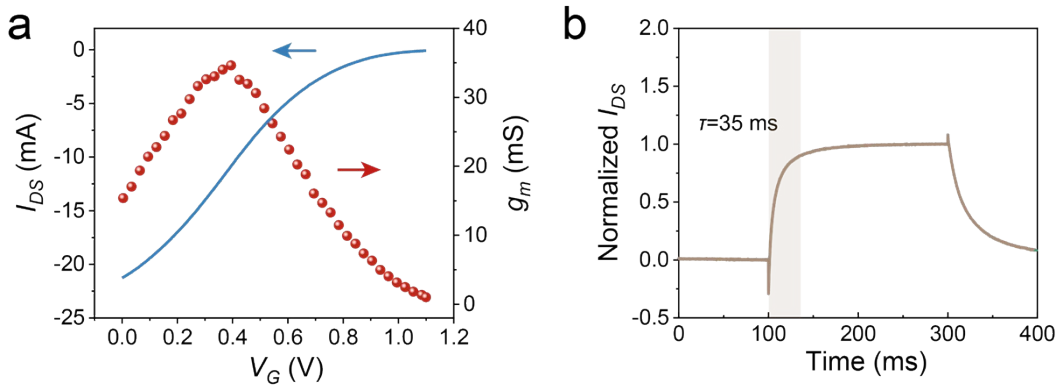

Fig. S13. (a) Transfer (solid line) and transconductance (sphere symbol) curves of the slow-response OECT. (b) Response behavior of the slow-response OECT. The rectangular shadow represents the response time of 35 ms.

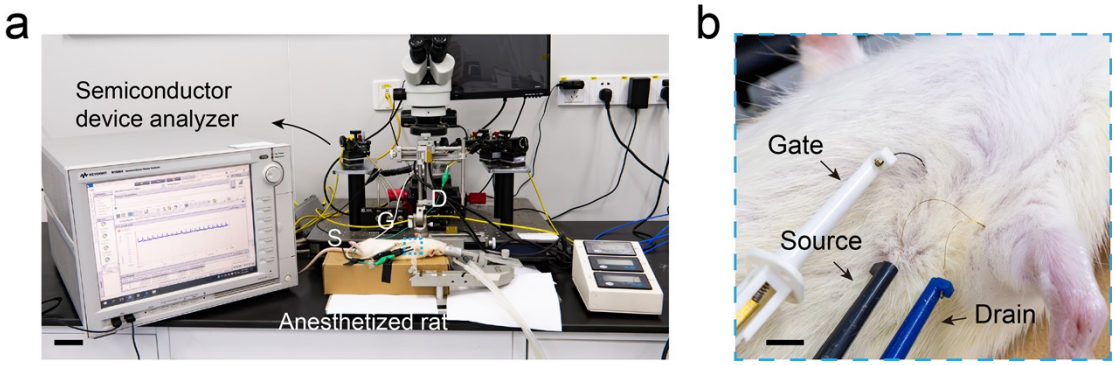

Fig. S14. ECG monitoring system setup. (a) Overview photograph of the ECG monitoring system. Scale bar, 5 cm. (b) Detailed photograph illustrating the connection of the implanted F-vOECT with the monitoring system. Scale bar, 5 mm.

Table S1. Comparison of response time of this work with the planar OECTs for ECG monitoring.

Morphology	Response time	Application	Ref.
Plane	1.5 ms	ECG (Epidermal)	*Adv. Mater.*, 2014, **26**, 3874-3878.
Plane	60 μs	ECG (rat heart *in vivo*)	*Sci. Adv.*, 2018, **4**, eaau2426.
Plane	361-636 μs	ECG (Epidermal)	*ACS Appl. Electron. Mater.*, 2020, **2**, 3601-3609.
Plane	40.57 μs	ECG (Epidermal)	*ACS Nano*, 2022, **16**, 12049-12060.
Plane	8.3 ms	ECG (Epidermal)	*Adv. Funct. Mater.*, 2022, **32**, 2200458.
Plane	10 μs	ECG (Epidermal)	*Sci. Adv.*, 2023, **9**, eadd9627.
Plane	6.67 ms	ECG (Epidermal)	*Nat. Electron.*, 2023, **6**, 281-291.
Plane	108 μs	ECG (Epidermal)	*Adv. Funct. Mater.*, 2023, **33**, 2209354.
Plane	12.9 ms	ECG (Isolated rat heart)	*Science,* 2023, **381**, 686-693.
Plane	16 ms	ECG (Epidermal)	*Adv. Mater. Technol.,* 2023, **8**, 2200611.
Plane	15.2 ms	ECG (Simulate)	*Chem. Mater.*, 2024, **36**, 1841-1854.
Fiber	**12 ms**	**ECG (Subcutaneous)**	**This work**

Table S2. Comparison of response time and V_G ($g_{m,\ max}$) of this work with other fiber OECTs.

Response time (s)	V_G ($g_{m,\ max}$) (V)	Ref.
0.1	0.69	*Sci. China. Chem.,* 2020, **63**, 1281-1288.
0.34	1	*ACS Appl. Mater. Interfaces,* 2019, **11**, 13105-13113.
0.5	0.19	*Biosens. Bioelectron.,* 2017, **95**, 138-145.
0.6	0.65	*Mater. Sci. Eng., B,* 2022, **278**, 115657.
0.64	0.873	*Adv. Fiber Mater.,* 2023, **5**, 1025-1036.
0.85	0.27	*Nano Res.,* 2023, **16**, 11885-11892.
1.4	0.17	*Electrochim. Acta,* 2022, **425**, 140716.
0.2	0.1	*npj Flexible Electron.,* 2022, **6**, 31.
0.5	1.15	*Anal. Bioanal. Chem.,* 2020, **412**, 7515-7524.
0.012	**0**	**This work**